THE JOURNAL OF PHYSICAL CHEMISTRY C

Article

pubs.acs.org/JPCC

Improvement of Hydrogen Vacancy Diffusion Kinetics in MgH_2 by Niobium- and Zirconium-Doping for Hydrogen Storage Applications

Estefania German*[,†,‡] and Ralph Gebauer[‡]

[†]Departamento de Física, Universidad Nacional del Sur & IFISUR (UNS-CONICET), Av. Alem 1253, 8000, Bahía Blanca, Argentina

[‡]The Abdus Salam International Center for Theoretical Physics (ICTP), Strada Costiera 11, 34151, Trieste, Italy

ABSTRACT: Transition metal (TM) catalytic dopants are broadly used in hydrogen storage materials to increase H_2 desorption and absorption kinetics. We have studied H vacancy formation energy in pure, Nb- or Zr- doped bulk magnesium hydride using density functional theory based calculations. The preferential dopant location was determined by means of occupation energy analysis. Both TM species prefer substitutional locations, Zr being more stable than Nb. Five different sites for H vacancy formation have been considered, all of them near the dopant. The vacancy formation energy decreases, especially in the interstitial Zr system in comparison with a pure one (from 1.35 to 0.51 eV). Concerning diffusion, we consider four paths in the pure and doped systems: the doping with TMs diminishes the activation energy barriers improving the diffusion kinetics, being more considerable for Zr. Effects of a possible spin polarization induced in the system by TM atoms and H vacancies generation have been considered as well.

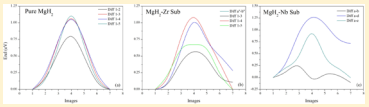

1. INTRODUCTION

Hydrogen is considered a very promising energy vector. Among its attractive features are a high gravimetric energy content and the possibility of zero CO_2 emissions when used in conjunction with a fuel cell.[1,2] The most significant problem which hydrogen faces for mobile applications concerns its storage.[3,4] The challenge is to find materials that can efficiently store hydrogen and that also present appropriate kinetics for the absorption and release of hydrogen.

MgH_2 attracts a lot of attention as one of the most practical solutions for on-board storage, due to its high hydrogen capacity and low cost.[5] However, its slow hydrogenation and dehydrogenation kinetics, the stability of Mg−H bonds and the required high temperature of about 300 °C for decomposition are prime obstacles for mobile applications.[6,7]

Various attempts have been made to improve the magnesium hydride absorption/desorption properties. Diffusion in solids is mediated by point defects; therefore it is essential to understand the defect physics as well as the migration mechanisms and barriers in MgH_2.[8−12]

Improvement of the hydrogen absorption/desorption kinetics is achieved through shortening the path for H diffusion (nanostructures, thin films) or by introducing appropriate dopants which act as catalysts.[13,14] In the last years, research has focused on the use of transition metals (TM) as dopants. TMs are considered good candidates to change the hydrogen diffusion kinetics and the stability of MgH_2.[2,15−25] The TM influences the stability of the MgH_2 and causes weakening of the Mg−H bonds. Consequently, TM doping leads to a variation of the cell volume. In literature one can find several corresponding experimental studies. For instance, C.X. Shang et al.[26] used mechanical alloying (MA) to process powder mixtures of MgH_2 with 8 mol % M (M = Al, Ti, Fe, Ni, Cu and Nb) in order to modify hydrogen storage properties of the Mg hydride. Dehydrogenation at 300 °C under vacuum shows that the (MgH_2+Ni) mixture gives the highest level of hydrogen desorption and the fastest kinetics, followed by MgH_2 doped with Al, Fe, Nb, Ti, and Cu. In addition, G. Liang and co-workers[27] have used intensive mechanical milling to make MgH_2−TM (TM = Ti, V, Mn, Fe, Ni) nanocomposite powders and have evaluated their hydrogen storage properties. The five 3d-elements showed different catalytic effects on the reaction kinetics. Desorption was most rapid for MgH_2−V, followed by MgH_2−Ti, MgH_2−Fe, MgH_2−Ni, and MgH_2−Mn at low temperatures. The activation energy of desorption for magnesium hydride was reduced drastically by milling with transition metals. Theoretically, Hussain et al.[28] have studied the structural, electronic, and hydrogen desorption properties of MgH_2 substituted by selected TMs (Sc, V, Fe, Co, Ni, Cu, Y, Zr and Nb), which substitute for Mg at a doping concentration of 3.125%. They concluded that doping with certain TMs can facilitate desorption of hydrogen from MgH_2 at much lower temperatures than from their pure forms.

Here, we have selected Nb and Zr as TM dopants because of the existence of various experimental studies. A theory-derived microscopic view will help to better understand the reaction mechanism. Even though Pd and Pt are catalyst candidates of excellence, it is an important goal to find cheaper and more accessible alternatives.

Experimentally, MgH_2−Nb systems have been studied by several techniques like scanning electron microscopy (SEM),[29−31] X-ray diffraction (XRD),[29−33] transmission electron microscopy (TEM),[31,32] analysis of real-time synchrotron X-ray powder diffraction,[33] desorption kinetics by Sievert-type apparatus,[29] dehydrogenation behavior by differential scanning calorimetry (DSC), and the hydrogen content by

Received: December 10, 2015
Revised: January 19, 2016
Published: February 16, 2016

DOI: 10.1021/acs.jpcc.5b12092
J. Phys. Chem. C 2016, 120, 4806−4812

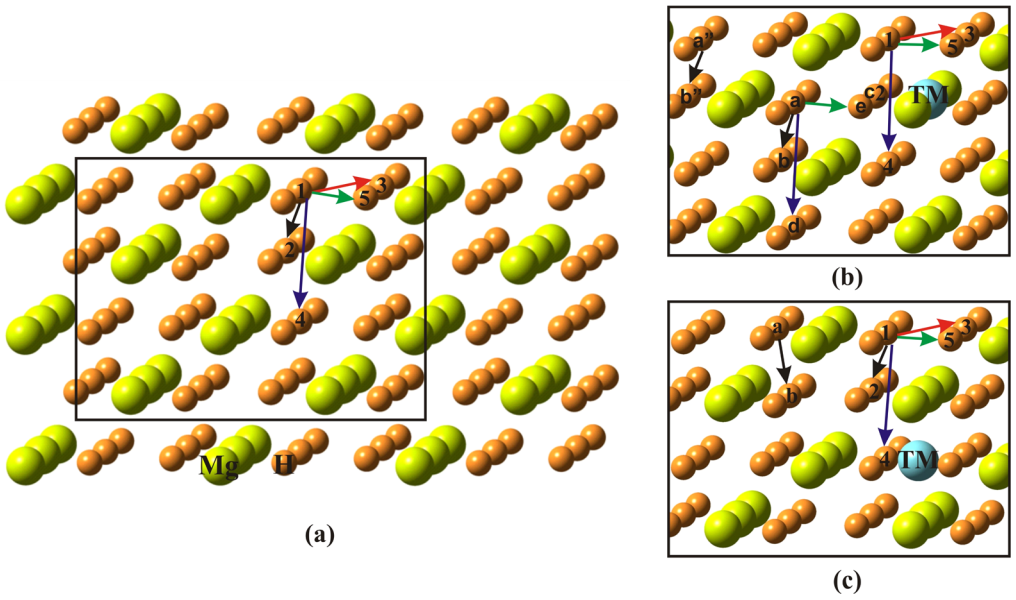

Figure 1. (a) MgH_2 supercell including labeling of hydrogen extracted to generate vacancies. (b) Zoomed view of the substituent TM location. (c) Zoomed view of the interstitial TM location. Labels 1 to 5 correspond to first neighbor H vacancies, labels *a* to *e* correspond to second neighbor, and labels *a″* to *b″* correspond to third neighbor H vacancies.

Leco determinator.[32] In these works, it was found that Nb catalyzes the dissociation of the Mg hydride. The rate limiting step in the MgH_2 dissociation is the atomic migration of H through the interconnected H−Mg layers. de Castro et al.[32] have investigated the structural evolution of Mg, Nb, and a mixture of Mg−5 at. % Nb processed by reactive milling (RM) carried out under a hydrogen atmosphere. Results revealed the RM Mg−Nb mixture presented a better dehydrogenation behavior when compared to pure Mg as a result of the catalytic effect of Nb. The Mg−Nb nanocomposite showed low desorption temperature and fast kinetics of hydrogen sorption. When Nb catalyst is added to Mg almost all material was transformed into hydride. The authors detected the presence of a NbH_2 phase in the RM Mg−Nb nanocomposite. This phase was not detected when pure Nb was milled under the same conditions. This result indicates that Mg promoted the hydrogenation of Nb in the same way that Nb promoted the hydrogenation of Mg.

There are only few studies concerning MgH_2−Zr systems. For instance, Malka et al.[34] have obtained MgH_2/NbF_5 and MgH_2/ZrF_4 materials by ball milling and found good hydrogen storage capacities. The hydrogen sorption stabilities evaluated using a volumetric Sieverts' apparatus showed good reversibility and performance for both materials. A better hydriding/dehydriding stability of MgH_2 was observed when modified by a ZrF_4 additive for cycling at 325 °C. Desorption kinetics of MgH_2 doped with TM (Nb, Fe and Zr) were studied by several techniques[35] showing that a few at. % concentrations of TMs catalyze the H_2 desorption process. H_2 desorption kinetics is stabilized after a few H_2 sorption cycles when TM atoms are aggregated, forming nanoclusters; mixed Fe and Zr additives produce faster H_2 desorption kinetics than a single additive. The effect of additives Ti, Pd, and Zr on the rate of hydrogen desorption from MgH_2 was investigated using high-pressure differential scanning calorimetry.[36] Enhanced dehydriding kinetics are obtained in the presence of Pd and Zr. The desorption rate for all the composites was found to increase with temperature as well as with the pressure difference between experimental and equilibrium pressures.

Here we report on computer simulations investigating the Nb and Zr doping in bulk MgH_2. Both Mg substitution by TMs and TM interstitials in MgH_2 were considered. The occupation energies, hydrogen vacancy formation energies and vacancy diffusion barriers, as well as the magnetic structure were calculated using density functional theory (DFT).

2. COMPUTATIONAL METHODOLOGY

All calculations were carried out in the framework of DFT using a plane-wave basis set as implemented in version 5.1 of the quantum-ESPRESSO suite of electronic structure codes.[37] The generalized gradient approximation (GGA) with the Perdew−Wang-91 (PW91) functional[38,39] was used throughout.

For geometry optimizations, crystal structure determined by Park et al.[40] and experimental data at room temperature for bulk MgH_2[41] were considered as starting structures. The electron−ion interactions were modeled using Vanderbilt's ultrasoft pseudopotentials (USPP)[42] (H.pw91-van_ak.UPF, Mg.pw91-np-van.UPF, Nb.pw91-nsp-van.UPF, Zr.pw91-nsp-van.UPF) available at the Quantum ESPRESSO Web site.[43] The employed pseudopotentials correspond to the following electronic configurations: $1s^2$ for H, $2p^6\ 3s^2$ for Mg, $4s^2\ 4p^6\ 4d^4\ 5s^1$ for Nb, and $4s^2\ 4p^6\ 4d^2\ 5s^2$ for Zr. This choice amounts to a valence of 1 for H, 8 for Mg, 13 for Nb and 12 for Zr.

A plane-wave cutoff energy of 35 Ry was used for the Kohn−Sham orbitals, and 350 Ry for the charge density. We checked that higher cutoff values did not affect significantly the results.

The studied structures were simulated using a supercell containing 162 atoms (27 unit cells of MgH_2; see Figure 1a). The Brillouin-zone was sampled using a 2 × 2 x 2 Monkhorst−Pack grid.[44]

The calculation of energy barriers and reaction pathway was carried out using the nudged elastic band (NEB) method.[45−49] For the NEB calculations, we used the Broyden optimizer to move the system under the NEB forces toward the minimum energy path (MEP). The climbing image algorithm was also

DOI: 10.1021/acs.jpcc.5b12092
J. Phys. Chem. C 2016, 120, 4806−4812

used with the NEB calculations to move the highest energy image toward the saddle point along the reaction coordinate. Seven images in total were used to explore the potential energy along the MEP. Forces were converged below 0.05 eV/Å.

In a previous work,[50] we calculated lattice parameters for the pristine MgH_2 cell, which has a rutile type tetragonal structure (P42/mnm, group No. 136), characterized by a lattice parameter a and the c/a ratio, a = 4.501 Å, c/a = 6.674, and u = 3.22 Å. These results are in close agreement with experimental values.

Here, TM dopants were added to the bulk considering two different configurations: TM as a substituent atom replacing a Mg atom (called Sub), and a TM atom located in an interstitial site (called Inter). Figure 1 shows the MgH_2 bulk and the location of dopants and H vacancies generated in the systems.

The occupation energy (E_{occ}) was calculated in order to identify the preferential site for dopants in the bulk and the relative stability of the doped system compared with pure MgH_2, using the following definition:

$$E_{occ} = E(Mg_{54-x}TM_{x+y}H_{108}) - [E(Mg_{54}H_{108}) + (x + y)E(TM) - xE(Mg)]$$

being (x = 1, y = 0) when TM substitutes a Mg atom and (x = 0, y = 1) when TM is located in an interstitial site, $E(Mg_{54-x}TM_{x+y}H_{108})$ is the total energy of the doped system, $E(Mg_{54}H_{108})$ is the energy of the pure MgH_2, E(TM) is the energy of the dopant calculated in a bulk divided by the number of atoms and E(Mg) is the energy of Mg calculated in a bulk divided by the number of atoms. As mentioned above, Hydrogen vacancies (vH) were also considered in the systems. The extracted atoms were first and second neighbors (fn and sn) of a TM. We also have calculated the formation energy of vacancies for the systems:

$$E_{vH} = E(Mg_{54-x}TM_{x+y}H_{108-1}) + 1/2E(H_2) - E(Mg_{54-x}TM_{x+y}H_{108})$$

being (x = 1, y = 0) when TM substitutes a Mg atom and (x = 0, y = 1) when TM is located in an interstitial site, as it was considered in the previous equation, $E(Mg_{54-x}TM_{x+y}H_{108-1})$ is the energy of the doped system containing a vH, E (H_2) is the energy of hydrogen gas and $E(Mg_{54-x}TM_{x+y}H_{108})$ is the energy of the doped system without vacancies. The model used is shown in Figure 1. We can see the MgH_2 cell containing 54 Mg atoms and 108 H atoms (a), the substitutional (b), and interstitial site (c), where the TM is located in the unit cell, and which H atoms were removed to model the vacancies.

To calculate the diffusion properties we have taken into account four different paths, the top four paths with minimum activation energy barriers, namely, from site 1 to 2 called diffusion 1−2, from site 1 to 3 called diffusion 1−3, from site 1 to 4 called diffusion 1−4 and from site 1 to 5 called diffusion 1−5 (see numbering in Figure 1), this correspond to first neighbor H atoms. The second neighbor analogous diffusions are called diffusion a−b (from vHa to vHb), diffusion a−c (from vHa to vHc), diffusion a−d (from vHa to vHd), and diffusion a−e (from vHa to vHe). In addition, the third neighbor analogous diffusion is called diffusion a″−b″ (from vHa" to vHb").

Systems with a hydrogen vacancy carry an odd number of electrons. For this reason, spin-polarized calculations were performed, which have also been used in cases where TM atoms are present.

The explicit treatment of spin polarization is crucial for the correct description of the electronic structure in these open-shell systems. In the following, we summarize the main magnetic features. For pure MgH_2 m = 0 μ_B because all orbitals are doubly occupied. Instead, if a H vacancy is generated, independently of its location, m = 1.00 μ_B due to the unpaired electron around the vacancy.

When a dopant is included in the system, magnetism is induced by the TM's d-electrons.

For MgH_2−Zr(Inter) m = 0.17 μ_B in the absence of H vacancies. When a H atom is extracted from the cell, m is approximately 1 μ_B: the lone electron around the vacancy pairs with one of the Zr $4d^2$ unpaired electrons, introducing a magnetization in the system of approximately 1 μ_B. This behavior is similar to the pure hydride.

In the case of MgH_2−Zr(sub), the magnetization value is 2.00 μ_B due to the two spin-aligned electrons in the TM's d-shell. When a H vacancy is generated the values of m are around 3 μ_B, 1 μ_B or 0 μ_B, depending on the location of the vacancy.

In the case of Nb, magnetism is also found in the hydride. When Nb is added to the bulk in an interstitial site m = 1.16 μ_B and when vacancies are generated the magnetism can take different values (approximately 0 μ_B, 1 μ_B, or 2 μ_B) depending on the vH location. In the substitutional case m = 3.00 μ_B and when H vacancies are present, m takes values around 0 and 2 μ_B.

The magnetic moment is more pronounced when the TM is substituting a Mg atom.

These magnetic characteristics are summarized in Table 1.

Table 1. Magnetization of Studied Systems[a]

	Magnetization (Bohr mag/cell)					
		vH1	**vH2**	**vH3**	**vH4**	**vH5**
pure MgH_2	0.00	1.00	1.00	1.00	1.00	1.00
MgH_2−Zr(inter)	0.17	0.90	0.99	1.16	1.13	0.90
MgH_2−Nb(inter)	1.16	0.16		0.99	0.00	0.16
		vHa	**vHb**			
		0.15	1.97			
		vH1	**vH2**	**vH3**	**vH4**	**vH5**
MgH_2−Zr(sub)	2.00	3.00		3.00	3.00	1.00
		vHa″	**vHb″**			
		1.00	3.00			
		vHa	**vHb**	**vHc**	**vHd**	**vHe**
MgH_2−Nb(sub)	3.00	0.68	1.87	2.00	0.00	0.68

[a]Pure MgH_2 and Zr- or Nb-doped MgH_2 with and without H vacancy.

3. RESULTS AND DISCUSSIONS

3.1. Geometry and Energy Optimization. The pristine MgH_2 bulk was relaxed in order to find the equilibrium geometry and energy. This was also done for the doped systems (MgH_2−Nb (inter), MgH_2−Nb (sub), MgH_2−Zr (inter), and MgH_2−Zr (sub)). In Table 2 the occupation energy and the energy needed to form the H vacancies (from vH1 to vH5) are listed.

The dopant occupation energy in the four cases is positive, this suggests that some energy is required to add a TM atom or substitute one Mg with one TM. Specifically, substitutional replacement is energetically more probable than a interstitial

DOI: 10.1021/acs.jpcc.5b12092
J. Phys. Chem. C 2016, 120, 4806−4812

Table 2. TM Occupation Energy (E_{occ}) and Hydrogen Vacancy Formation Energy (E_{vHx}) for MgH_2 Bulk Systems (in eV)

	pure MgH_2	MgH_2–Zr(inter)	MgH_2–Zr(sub)	MgH_2–Nb(inter)	MgH_2–Nb(sub)
E_{occ}		2.36	1.10	1.88	1.68
E_{vH1}	1.35	0.51	1.32	0.59	1.81
E_{vH2}	1.35	0.93	1.65	1.47	1.27
E_{vH3}	1.35	1.33	1.32	1.50	1.81
E_{vH4}	1.35	0.98	1.32	1.06	1.80
E_{vH5}	1.35	0.51	0.70	0.59	1.64

occupation in both cases, Zr and Nb dopants (1.10 and 1.68 eV, respectively). This is in agreement with previous studies where a preference for substitutional sites was found for a set of TM atoms in MgH_2 bulk and surfaces.[1,2,17,20,51,52] However, these results for the bulk system differ from our previous findings in MgH_2 (001) and (110) surfaces, where the preferential site was found to be an interstitial location.[25,53] We ascribe the different site preference of dopants to the varying coordination numbers of bulk versus surface sites. From experimental studies, no information is available yet about preferential locations of the dopants in the lattice and the influence of surfaces on the preferred dopant sites. We foresee that it will be possible to link the computed information presented here to experimental information indirectly, for example using kinetic Monte Carlo studies of diffusion processes in MgH_2. Work along those lines is currently in progress.

The hydrogen vacancy formation energy in the pure system is the same for the five different locations, 1.35 eV. This value is in agreement with other studies except for small differences due to the higher number of valence electrons considered in our calculation.[8,12,15,54,55] However, when these vacancies are generated in the Zr-doped systems, the vacancy formation energies decrease until values of 0.51 eV. On the contrary, in the case of Nb-doped systems this energy increases in most cases, strong Nb–H bonds are present in the cell making it more difficult to break the bond and release the H atom. In order to promote the hydrogenation/dehydrogenation process, a balance between occupation energy and vacancy formation energy must be found. Substitutional Zr-doped systems seem to be the most appropriate ones, due to the lowest occupation energy and the ease to generate H vacancies.

3.2. H Vacancy Diffusion. In order to study the diffusion of a H vacancy in the MgH_2 crystal four reaction paths were considered, namely, diffusion 1–2, diffusion 1–3, diffusion 1–4 and diffusion 1–5; see Figure 1.

In the case of pristine MgH_2, the H vacancy formation energy is the same for the five locations. In the doped systems this vacancy formation energy is in some cases lower and in other cases higher than in pure MgH_2, depending on the kind of dopant and the relative positions of vacancy and TM. For the analysis of the diffusion kinetics, we considered the migration of H vacancies between the positions which are energetically most favorable. For this purpose we have also calculated the H vacancy formation energy for H atoms which are more distant from the TM atoms, i.e., second neighbors (sn) and third neighbors (tn). These values are resumed in Table 3 (see labeling in Figure 1). It was not necessary to calculate sn H vacancy for MgH_2–Zr (int) because the fn H vacancies are already easy to form for this case (see Table 2).

MgH_2–Nb(sub) vHd vacancy still needs more energy to be generated than in the pure system, nonetheless this vacancy is used in the calculation of diffusion a-d because the initial state

Table 3. Second (and Third) Neighbor Hydrogen Vacancy Formation Energy (E_{vHx}) in eV

MgH_2–Zr(sub)		MgH_2–Nb(inter)	MgH_2–Nb(sub)
$E_{vHa''}$ 1.31	E_{vHa}	1.34	1.16
$E_{vHb''}$ 1.34	E_{vHb}	1.16	1.07
	E_{vHc}	1.50	1.27
	E_{vHd}		1.87
	E_{vHe}		1.16

vHa is easier to generate than vH1 (diffusions occur from fn to fn or from sn to sn). In the case of Nb the generation of sn vacancies requires less energy because the strong Nb–H bonds weakens the further Mg–H bonds, allowing the desorption.

First, we concentrate on the case of substitutional doping for the study of the diffusion because this configuration is energetically more favorable than interstitial TM doping. Also, the generation of H vacancies requires less energy in these cases.

In Table 4 activation energy barriers are listed. The energy for the pristine MgH_2 system reported here is slightly different from previous results.[11,56,57] This difference is due to the fact that we consider 8 valence electrons for Mg (which is more precise), while only two valence electrons have been modeled in the previous mentioned studies. From values on Table 4 we can observe a lowering of the diffusion barriers in the cases of diffusion a″–b″, diffusion 1–4, and diffusion 1–5 for MgH_2–Zr (sub) and of diffusion a–b and diffusion a–e in MgH_2–Nb (sub), in comparison with pristine MgH_2. No values are reported for diffusion a–c in MgH_2–Nb (sub) because no stable diffusion path was found for this case. In Figure 2 the vH diffusion curves for pure MgH_2, MgH_2–Zr (sub), and MgH_2–Nb (sub) are shown. The curves for the pure system are symmetric because in the absence of dopants the initial and final states are geometrically equivalent. In Figure 2b, diffusion 1–5 was calculated considering a new initial state with a different geometrical configuration which makes possible the diffusion. The diffusion energy curves were shifted to zero energy for the first image in order to better compare activation energies.

Let us now consider the diffusion energy barriers in the case of interstitial TMs. From Table 5 we can see that the most substantial improvement in the kinetics is for diffusion 1–4 and 1–5 in MgH_2–Zr (inter), where the activation energy is reduced by 30% with respect to pristine MgH_2. For MgH_2–Nb (inter) only slight improvements are found for just one direction of the considered diffusion paths. In Figure 3 the vH diffusion curves for pure MgH_2 (as reference), MgH_2–Zr (inter) and MgH_2–Nb (inter) are plotted. It can be seen the significant lowering in the activation barriers for diffusion 1–4 and 1–5 in MgH_2–Zr (inter).

DOI: 10.1021/acs.jpcc.5b12092
J. Phys. Chem. C 2016, 120, 4806–4812

Table 4. Activation Energy Barriers for Diffusions of H Vacancies in Pure and Substitutional Doped MgH_2 Systems[a]

pure MgH_2		MgH_2–Zr(sub)			MgH_2–Nb(sub)		
			A → B	B → A		A → B	B → A
diffusion 1–2	0.79	diffusion a″–b″	0.56	0.46	diffusion a–b	0.24	0.34
diffusion 1–3	1.06	diffusion 1–3	1.08	1.08	diffusion a–c	–	–
diffusion 1–4	1.05	diffusion 1–4	0.67	0.67	diffusion a–d	1.29	0.55
diffusion 1–5	1.10	diffusion 1–5	1.01	0.73	diffusion a–e	0.92	0.93

[a]All energies are expressed in eV.

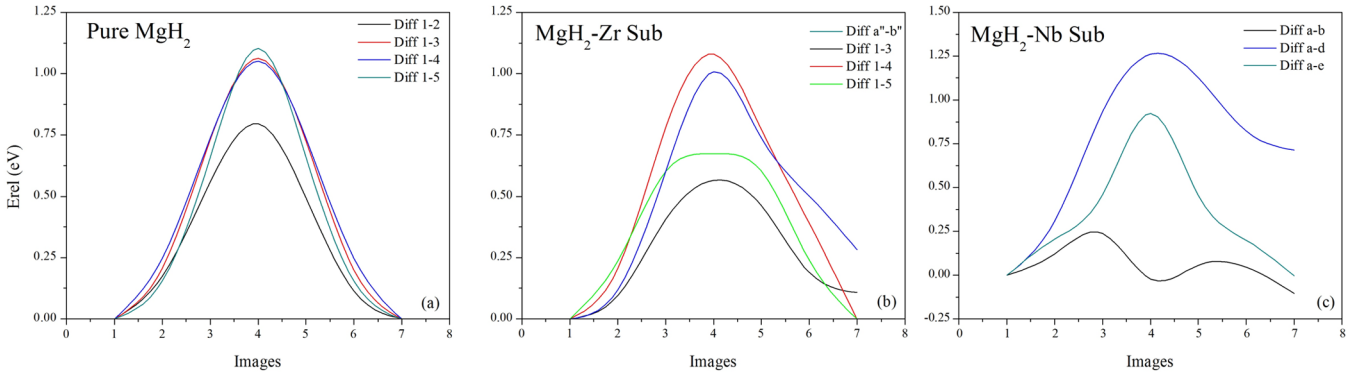

Figure 2. vH diffusion curves for (a) pure MgH_2, (b) MgH_2–Zr (sub), and (c) MgH_2–Nb (sub).

Table 5. Activation Energy Barriers for Diffusions of H Vacancies in Pure and Interstitial Doped MgH_2 Systems[a]

pure MgH_2		MgH_2–Zr(int)			MgH_2–Nb(int)		
			A → B	B → A		A → B	B → A
diffusion 1–2	0.79	diffusion 1–2	1.27	0.86	diffusion a–b	0.62	0.97
diffusion 1–3	1.06	diffusion 1–3	1.47	0.65	diffusion 1–3	1.26	0.35
diffusion 1–4	1.05	diffusion 1–4	0.74	0.28	diffusion 1–4	1.14	0.67
diffusion 1–5	1.10	diffusion 1–5	0.58	0.58	diffusion 1–5	1.67	1.67

[a]All energies are expressed in eV.

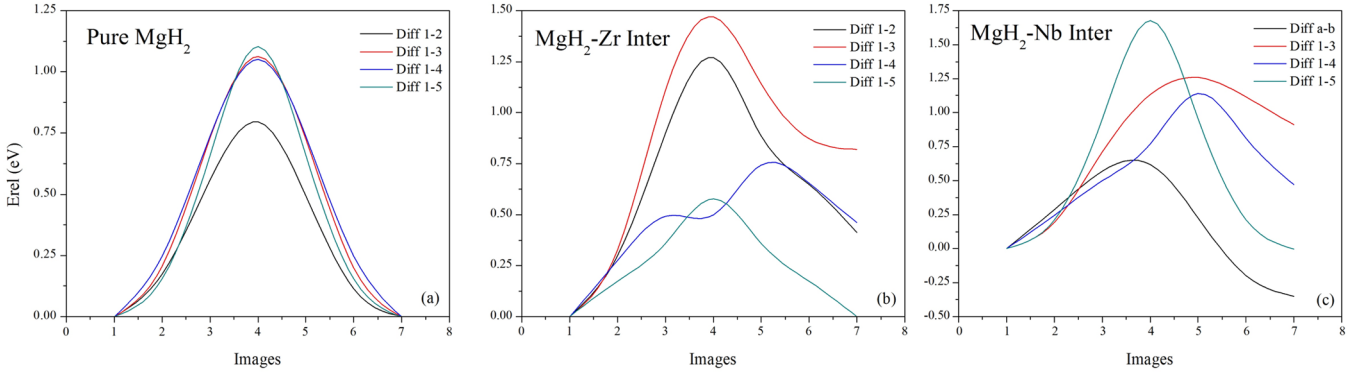

Figure 3. Four vH diffusion curves for (a) pure MgH_2, (b) MgH_2–Zr (inter), and (c) MgH_2–Nb (inter).

4. CONCLUSION

We performed first principle electronic structure calculations of pure bulk MgH_2 and MgH_2 containing Nb and Zr dopants in two different positions, namely, substitutional and interstitial location. We analyzed the dopant occupation energy as well as hydrogen vacancy formation energy and its diffusion in the systems. In addition, spin-polarized calculations were performed to take into account a possible magnetic influence of TM impurity on the MgH_2 properties.

Our calculations show that Nb and Zr dopants prefer substitutional instead of interstitial location; however, the energetic difference between locations is not that large. First neighbor hydrogen vacancies are easier to generate when the MgH_2 is doped with Zr, and second neighbor hydrogen vacancies when MgH_2 is doped with Nb.

The energy barrier in the hydrogen vacancy diffusion is reduced between 16% and 73% in the doped systems. TM addition forms TM-H bonds which weaken the surrounding Mg–H bonds, thus destabilizing the structure. We can deduce that Nb–H formed bonds are stronger than Zr–H ones because in order to calculate the diffusion we needed to involve atoms which are further from the Nb atom, the surrounding Hs are more difficult to extract than second neighbor Hs. Larger

DOI: 10.1021/acs.jpcc.5b12092
J. Phys. Chem. C 2016, 120, 4806–4812

magnetic moments appeared in the doped systems due to the presence of d-electrons of TM atoms.

AUTHOR INFORMATION

Corresponding Author

*(E.G.) egerman@uns.edu.ar. Telephone: +54 291 4882982 int. 33.

Notes

The authors declare no competing financial interest.

ACKNOWLEDGMENTS

E.G. is a member of CONICET. The authors acknowledge SGCyT (UNS), IFISUR-CONICET, CIC-Buenos Aires, PICT 1770, and PICT-2012-1609 for financial support. E.G. would like to thank the ICTP and the Simons Foundation for providing the opportunity to undertake this research by supporting her visit to the ICTP as an ICTP−Simons Associate. We thank useful discussions with Dr. Valeria Verdinelli.

REFERENCES

(1) Dai, J. H.; Song, Y.; Yang, R. Intrinsic Mechanisms on Enhancement of Hydrogen Desorption from MgH_2 by (001) Surface Doping. *Int. J. Hydrogen Energy* **2011**, *36*, 12939−12949.

(2) Dai, J. H.; Song, Y.; Yang, R. First Principles Study on Hydrogen Desorption from a Metal (=Al, Ti, Mn, Ni) Doped MgH_2 (110) Surface. *J. Phys. Chem. C* **2010**, *114*, 11328−11334.

(3) Aguey-Zinsou, K.-F.; Ares-Fernández, J. R. Hydrogen in Magnesium: New Perspectives Toward Functional Stores. *Energy Environ. Sci.* **2010**, *3*, 526−543.

(4) Blagojević, V. A.; Minić, D. G.; Novaković, J. G.; Minić, D. M., Ed. by *Hydrogen Energy - Challenges and Perspectives*; Minić, D., Ed.; InTech: 2012; Chapter 1. DOI: 10.5772/46098.

(5) Jain, I. P.; Lal, C.; Jain, A. Hydrogen Storage in Mg: A Most Promising Material. *Int. J. Hydrogen Energy* **2010**, *35*, 5133−5144.

(6) Schlapbach, L.; Züttel, A. Hydrogen-Storage Materials for Mobile Applications. *Nature* **2001**, *414*, 353−358.

(7) Bogdanović, B.; Bohmhammel, K.; Christ, B.; Reiser, A.; Schlichte, K.; Vehlen, R.; Wolf, U. Thermodynamic Investigation of the Magnesium−Hydrogen System. *J. Alloys Compd.* **1999**, *282*, 84−92.

(8) Park, M. S.; Janotti, A.; Van de Walle, C. G. Formation and Migration of Charged Native Point Defects in MgH_2: First-Principles Calculations. *Phys. Rev. B: Condens. Matter Mater. Phys.* **2009**, *80* (6), 064102.

(9) Lakhal, M.; Bhihi, M.; Labrim, H.; Benyoussef, A.; Naji, S.; Belhaj, A.; Khalil, B.; Abdellaoui, M.; Mounkachi, O.; Loulidi, M. El kenz, A. Kinetic Monte Carlo and Density Functional Study of Hydrogen Diffusion in Magnesium Hydride MgH_2. *Int. J. Hydrogen Energy* **2013**, *38*, 8350−8356.

(10) Hao, S.; Sholl, D. S. Selection of Dopants to Enhance Hydrogen Diffusion Rates in MgH_2 and $NaMgH_3$. *Appl. Phys. Lett.* **2009**, *94*, 171909.

(11) Du, A. J.; Smith, S. C.; Lu, G. Q. First-Principle Studies of the Formation and Diffusion of Hydrogen Vacancies in Magnesium Hydride. *J. Phys. Chem. C* **2007**, *111*, 8360−8365.

(12) Tao, S. X.; Kalisvaart, W. P.; Danaie, M.; Mitlin, D.; Notten, P. H. L.; van Santen, R. A.; Jansen, A. P. J. First Principle Study of Hydrogen Diffusion in Equilibrium Rutile, Rutile with Deformation Twins and Fluorite Polymorph of Mg Hydride. *Int. J. Hydrogen Energy* **2011**, *36*, 11802−11809.

(13) Grzech, A.; Lafont, U.; Magusin, P. C. M. M.; Mulder, F. M. Microscopic Study of TiF_3 as Hydrogen Storage Catalyst for MgH_2. *J. Phys. Chem. C* **2012**, *116*, 26027−26035.

(14) Liu, T.; Wang, C.; Wu, Y. Mg-based Nanocomposites with Improved Hydrogen Storage Performances. *Int. J. Hydrogen Energy* **2014**, *39*, 14262−14274.

(15) Koteski, V.; Belošević-Čavor, J.; Batalović, K.; Radaković, J.; Umićević, A. Hydrogen Diffusion in MgH_2 Doped with Ti, Mn and Fe. *RSC Adv.* **2015**, *5*, 34894−34899.

(16) Hussain, T.; Maark, T. A.; Pathak, B.; Ahuja, R. Improvement in the Hydrogen Desorption from MgH_2 upon Transition Metals Doping: A Hybrid Density Functional Calculations. *AIP Adv.* **2013**, *3*, 102117.

(17) Wang, L. L.; Johnson, D. D. Hydrogen Desorption from Ti-Doped MgH_2(110) Surfaces: Catalytic Effect on Reaction Pathways and Kinetic Barriers. *J. Phys. Chem. C* **2012**, *116*, 7874−7878.

(18) Hussain, T.; De Sarkar, A.; Maark, T. A.; Sun, W.; Ahuja, R. Strain and Doping Effects on the Energetics of Hydrogen Desorption from the MgH_2 (001) Surface. *EPL* **2013**, *101*, 27006.

(19) Novaković, N.; Grbović Novaković, J.; Matović, L.; Manasijević, M.; Radisavljević, I.; Paskaš Mamula, B.; Ivanović, N. Ab Initio Calculations of MgH_2, MgH_2:Ti and MgH_2:Co Compounds. *Int. J. Hydrogen Energy* **2010**, *35*, 598−608.

(20) Zeng, X. Q.; Cheng, L. F.; Zou, J. X.; Ding, W. J.; Tian, H. Y.; Buckley, C. Influence of 3d Transition Metals on the Stability and Electronic Structure of MgH_2. *J. Appl. Phys.* **2012**, *111*, 093720.

(21) Moser, D.; Bull, D. J.; Sato, T.; Noréus, D.; Kyoi, D.; Sakai, T.; Kitamura, N.; Yusa, H.; Taniguchi, T.; Kalisvaart, W. P.; Notten, P. Structure and Stability of High Pressure Synthesized Mg−TM Hydrides (TM = Ti, Zr, Hf, V, Nb and Ta) as Possible New Hydrogen Rich Hydrides for Hydrogen Storage. *J. Mater. Chem.* **2009**, *19*, 8150−8161.

(22) Xiao, X.-B.; Zhang, W.-B.; Yu, W.-Y.; Wang, N.; Tang, B.-Y. Energetics and Electronic Properties of Mg_7TMH_{16} (TM = Sc, Ti, V, Y, Zr, Nb): An Ab Initio Study. *Phys. B* **2009**, *404*, 2234−2240.

(23) Tao, S. X.; Notten, P. H. L.; van Santen, R. A.; Jansen, A. P. J. Fluorite Transition Metal Hydride Induced Destabilization of the MgH_2 System in MgH_2/TMH_2 Multilayers (TM = Sc, Ti, V, Cr, Y, Zr, Nb, La, Hf). *Phys. Rev. B: Condens. Matter Mater. Phys.* **2010**, *82*, 125448.

(24) Song, Y.; Guo, Z. X.; Yang, R. Influence of Selected Alloying Elements on the Stability of Magnesium Dihydride for Hydrogen Storage Applications: A First-Principles Investigation. *Phys. Rev. B: Condens. Matter Mater. Phys.* **2004**, *69*, 094205.

(25) Germán, E.; Verdinelli, V.; Luna, C. R.; Juan, A.; Sholl, D. A Theoretical Study of the Effect of Zr-, Nb-Doped and Vacancy-like Defects on H Desorption on MgH_2 (110) Surface. *J. Phys. Chem. C* **2014**, *118*, 4231−4237.

(26) Shang, C. X.; Bououdina, M.; Song, Y.; Guo, Z. X. Mechanical Alloying and Electronic Simulations of (MgH_2+M) Systems (M = Al, Ti, Fe, Ni, Cu and Nb) for Hydrogen Storage. *Int. J. Hydrogen Energy* **2004**, *29*, 73−80.

(27) Liang, G.; Huot, J.; Boily, S.; Van Neste, A.; Schulz, R. Catalytic Effect of Transition Metals on Hydrogen Sorption in Nanocrystalline Ball Milled MgH_2−Tm (Tm = Ti, V, Mn, Fe and Ni) Systems. *J. Alloys Compd.* **1999**, *292*, 247−252.

(28) Hussain, T.; Maark, T. A.; Chakraborty, S.; Ahuja, R. Improvement in Hydrogen Desorption from β-and γ-MgH_2 upon Transition-Metal Doping. *ChemPhysChem* **2015**, *16*, 2557−2561.

(29) Bazzanella, N.; Checchetto, R.; Miotello, A. Catalytic Effect on Hydrogen Desorption in Nb-doped Microcrystalline MgH_2. *Appl. Phys. Lett.* **2004**, *85*, 5212−5214.

(30) Shang, C.; Bououdina, M.; Guo, Z. X. Structural Stability and Dehydrogenation of (MgH_2+Al, Nb) Powder Mixtures during Mechanical Alloying. *Mater. Trans.* **2003**, *44*, 2356−2362.

(31) Cui, J.; Liu, J.; Wang, H.; Ouyang, L.; Sun, D.; Zhu, M.; Yao, X. Mg−TM (TM: Ti, Nb, V, Co, Mo or Ni) Core−Shell like Nanostructures: Synthesis, Hydrogen Storage Performance and Catalytic Mechanism. *J. Mater. Chem. A* **2014**, *2*, 9645−9655.

(32) de Castro, J. F. R.; Santos, S. F.; Costa, A. L. M.; Yavari, A. R.; Botta F, W. J.; Ishikawa, T. T. Structural Characterization and

DOI: 10.1021/acs.jpcc.5b12092
J. Phys. Chem. C 2016, 120, 4806−4812

Dehydrogenation Behavior of Mg−5 at.%Nb Nano-Composite Processed by Reactive Milling. *J. Alloys Compd.* **2004**, *376*, 251−256.
(33) Huot, J.; Pelletier, J. F.; Lurio, L. B.; Sutton, M.; Schulz, R. Investigation of Dehydrogenation Mechanism of MgH_2−Nb Nanocomposites. *J. Alloys Compd.* **2003**, *348*, 319−324.
(34) Malka, I. E.; Bystrzycki, J.; Płociński, T.; Czujko, T. Microstructure and Hydrogen Storage Capacity of Magnesium Hydride with Zirconium and Niobium Fluoride Additives after Cyclic Loading. *J. Alloys Compd.* **2011**, *509*, S616−S620.
(35) Bazzanella, N.; Checchetto, R.; Miotello, A. Atoms and Nanoparticles of Transition Metals as Catalysts for Hydrogen Desorption from Magnesium Hydride. *J. Nanomater.* **2011**, *2011*, 1−11.
(36) Berlouis, L. E. A.; Honnor, P.; Hall, P. J.; Morris, S.; Dodd, S. B. An Investigation of the Effect of Ti, Pd and Zr on the Dehydriding Kinetics of MgH_2. *J. Mater. Sci.* **2006**, *41*, 6403−6408.
(37) Giannozzi, P.; Baroni, S.; Bonini, N.; Calandra, M.; Car, R.; Cavazzoni, C.; Ceresoli, D.; Chiarotti, G. L.; Cococcioni, M.; Dabo, I.; et al. QUANTUM ESPRESSO: A Modular and Open-Source Software Project for Quantum Simulations of Materials. *J. Phys.: Condens. Matter* **2009**, *21*, 395502.
(38) Perdew, J. P.; Wang, Y. Accurate and Simple Analytic Representation of the Electron-Gas Correlation Energy. *Phys. Rev. B: Condens. Matter Mater. Phys.* **1992**, *45*, 13244−13249.
(39) Perdew, J. P. In *Electronic Structure of Solids*Ziesche, P., Eschrig, H., Eds.; Akademie Verlag: Berlin, 1991.
(40) Park, M. S.; Janotti, A.; Van de Walle, C. G. Formation and Migration of Charged Native Point Defects in MgH_2: First-Principles Calculations. *Phys. Rev. B: Condens. Matter Mater. Phys.* **2009**, *80*, 064102.
(41) Bortz, M.; Bertheville, B.; Böttger, G.; Yvon, K. Structure of the High Pressure Phase γ-MgH_2 by Neutron Powder Diffraction. *J. Alloys Compd.* **1999**, *287*, L4−L6.
(42) Vanderbilt, D. Soft Self-Consistent Pseudopotentials in a Generalized Eigenvalue Formalism. *Phys. Rev. B: Condens. Matter Mater. Phys.* **1990**, *41*, 7892−7895.
(43) http://www.quantum-espresso.org/pseudopotentials/.
(44) Monkhorst, H. J.; Pack, J. D. Special Points for Brillouin-Zone Integrations. *Phys. Rev. B* **1976**, *13*, 5188−5192.
(45) Jónsson, H.; Mills, G.; Jacobsen, K. W. In *Nudged Elastic Band Method for Finding Minimum Energy Paths of Transitions, in Classical and Quantum Dynamics in Condensed Phase Simulations*; Berne, B. J., Ciccotti, G., Coker, D. F., Eds.; World Scientific: 1998.
(46) Sheppard, D.; Terrell, R.; Henkelman, G. Optimization Methods for Finding Minimum Energy Paths. *J. Chem. Phys.* **2008**, *128*, 134106.
(47) Henkelman, G.; Jóhannesson, G.; Jónsson, H. In *Methods for Finding Saddle Points and Minimum Energy Paths, in Progress on Theoretical Chemistry and Physics*; Schwartz, S. D., Ed.; Kluwer Academic Publishers: 2000.
(48) Henkelman, G.; Uberuaga, B. P.; Jónsson, H. A Climbing Image Nudged Elastic Band Method for Finding Saddle Points and Minimum Energy Paths. *J. Chem. Phys.* **2000**, *113*, 9901−9904.
(49) Henkelman, G.; Jónsson, H. Improved Tangent Estimate in the Nudged Elastic Band Method for Finding Minimum Energy Paths and Saddle Points. *J. Chem. Phys.* **2000**, *113*, 9978−9985.
(50) Luna, C. R.; Germán, E.; Macchi, C.; Juan, A.; Somoza, A. On the Perfect MgH_2(−Nb,−Zr) Systems and the Influence of Vacancy-Like Defects on their Structural Properties. A Self-Consistent First Principle Calculations Study of the Electron and Positron Parameters. *J. Alloys Compd.* **2013**, *556*, 188−197.
(51) Giusepponi, S.; Celino, M. DFT Model of Hydrogen Desorption from MgH_2: The Role of Iron Catalyst. *Int. J. Hydrogen Energy* **2013**, *38*, 15254−15263.
(52) Larsson, P.; Araújo, C. M.; Larsson, J. A.; Jena, P.; Ahuja, R. Role of Catalysts in Dehydrogenation of MgH_2 Nanoclusters. *Proc. Natl. Acad. Sci. U. S. A.* **2008**, *105*, 8227−8231.
(53) Germán, E.; Luna, C.; Marchetti, J.; Jasen, P.; Macchi, C.; Juan, A. A DFT Study of Dopant (Zr, Nb) and Vacancies on the Dehydrogenation on MgH_2 (001) Surface. *Int. J. Hydrogen Energy* **2014**, *39*, 1732−1739.
(54) Stier, W.; Camargo, L. G.; Óskarsson, F.; Jónsson, H. Hydrogen Storage in Magnesium Based Alloys. *Prepr. Pap.-Am. Chem. Soc., Div. Fuel Chem.* **2005**, *50*, 15.
(55) Grau-Crespo, R.; Smith, K. C.; Fisher, T. S.; de Leeuw, N. H.; Waghmare, U. V. Thermodynamics of Hydrogen Vacancies in MgH_2 from First-Principles Calculations and Grand-Canonical Statistical Mechanics. *Phys. Rev. B: Condens. Matter Mater. Phys.* **2009**, *80*, 174117.
(56) Ming, W.; Fang, Z. Z.; Liu, F. Effects of Li Doping on H-Diffusion in MgH_2: A First-Principles Study. *J. Appl. Phys.* **2013**, *114*, 243502.
(57) Roy, A.; Janotti, A.; Van de Walle, C. G. Effect of Transition-Metal Additives on Hydrogen Desorption Kinetics of MgH_2. *Appl. Phys. Lett.* **2013**, *102*, 033902.

DOI: 10.1021/acs.jpcc.5b12092
J. Phys. Chem. C 2016, 120, 4806−4812